MOLECULAR PHYSICS REPORTS **38** (2003) 30-46

MAGNETISM IN LOW-DIMENSIONAL CUPRATES

K.-H. MÜLLER

IFW Dresden, POB 270016, D-01171 Dresden, Germany

Abstract: The interest in quasi low-dimensional cuprates originated from the discovery of high-T_c superconductors typically consisting of intermediate valence copper oxide planes. Usually the magnetism of the cuprates originates from the *d*-electrons of copper in the oxidation state Cu^{II}. In an ionic approximation the Cu^{II} species are described by Cu^{2+}. Its paramagnetic moment is well approximated by the spin-only value of 1.73 Bohr magnetons. A certain overlap of wave functions results in exchange interactions of the magnetic moments. The dominating type of interaction is superexchange *via* oxygen anions. In a more realistic description covalence or, more generally, overlapping electron wave functions combined with electron correlation have to be taken into account. In most cases the Cu^{II} cuprates contain quasi two-dimensional or quasi one-dimensional networks of CuO_4 plaquettes and they mostly behave like quantum spin - 1/2 antiferromagnets of low dimensionality ($D = 1$ or $D = 2$) whose macroscopic magnetic behaviour is governed by antiferromagnetic long-range order or spin singlet ground states. Weak interactions between low dimensional magnetic subsystems may lead to dimensionality crossover and quantum critical phenomena.

1. INTRODUCTION

The discovery of high-T_c superconductivity in the La-Ba-Cu-O system by Bednorz and Müller [1] led to a world wide effort to explore compounds containing copper oxide layers and related oxychlorides because they may become superconductors when doped. Figure 1 shows the crystal structure of (Ba, La)CuO_4 characterized by a network of corner-sharing CuO_4 plaquettes. Regarding the large spacing between the CuO_2 planes in the high-T_c cuprates and their electronic structure they can be considered as consisting of weakly interacting two-dimensional subsystems [2, 3]. Experimental data on the structural, electronic and magnetic properties of $La_{2-x}Sr_xCuO_4$ (which is similar to $La_{2-x}Ba_xCuO_4$) are summarized in the phase diagram of Fig. 2. Since La is expected to be always in the oxidation state (+3) and O in (-2) the electronic configuration of Cu in the undoped compound La_2CuO_4 is $3d^9$ with one hole per copper site. In a naive point of view such a material is expected to be a metal, but in reality it is an antiferromagnetic insulator because electron correlations prevent the charge fluctuations required for metallic conduction. Antiferromagnetic insulators of this type are called Mott-Hubbard insulators [2]. It is generally accepted that strong electron correlation has to be taken into account to understand phase diagrams as that of Fig. 2. And it has been even suggested that the correlations are responsible for the electron attractions which are required to obtain the high superconducting transition temperatures observed in the cuprate superconductors [4]. Figure 2 shows that, in particular at zero temperature, with increasing doping rate x various magnetic and electronic states occur which are separated by quantum critical points: Néel-type antiferromagnetism, spin glass, superconductivity and normal-state metallic behaviour. Additionally a quantum critical point is supposed to lie hidden within the superconducting range of x, separating a non-Landau-Fermi liquid in the underdoped range (small x) from a Landau-Fermi liquid [5]. Special characteristics of the underdoped range are pseudogap behaviour in the normal state and a cer-

tain type of electronic phase separation [6]. I.e. above the superconducting transition temperature the added holes tend to segregate into charge stripes which act like domain walls between antiferromagnetic regions. Those stripes have been observed by neutron scattering [7]. In La_2CuO_4 doped with Sr or Ba the added holes go predominantly into oxygen $2p$ dominated states because otherwise the Cu sites would be doubly occupied by holes [2, 8].

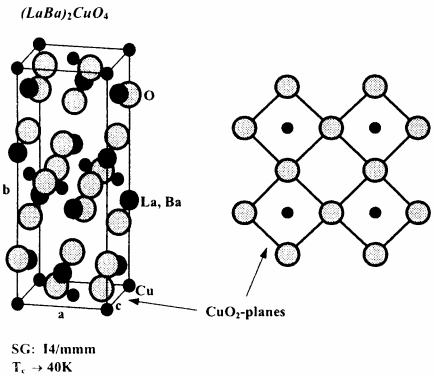

Fig. 1. Crystal structure of the high-T_c cuprate superconductor (La, Ba)$_2$CuO$_4$ [1] and the nearly planar CuO_2 network consisting of corner-sharing CuO_4-plaquettes. SG and T_c are the space group and the achieved superconducting transition temperature, respectively

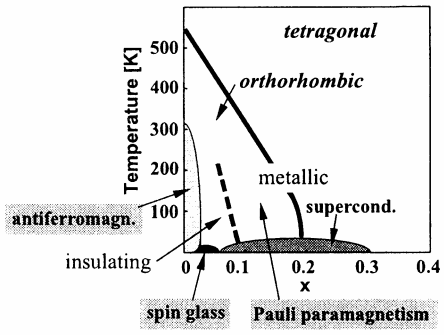

Fig. 2. Magnetic/electronic/structural composition-temperature phase diagram for $La_{2-x}Sr_xCuO_4$ (after [3]).

A similar phase diagram as that in Fig. 2, with antiferromagnetic and superconducting ground states, has been realized in $Nd_{2-x}Ce_xCuO_4$ i.e. by adding electrons instead of holes. To analyse the properties of cuprate superconductors the so called *t-J*-model, or some extended versions of it have successfully been used [2, 5]. This model has a simple chemical interpretation. The parent stoichiometric insulators have an oxidation state Cu^{II} corresponding to an $S = 1/2$ ion, and the magnetic interactions are well described by a simple next-neighbor Heisenberg model with a large value of the exhange interaction, $J/k_B \approx 1500$ K (see Section 2.2 below). Hole doping introduces the oxidation state Cu^{III} in the low spin configuration $S = 0$ (see Section 2.3). The Cu^{II} and Cu^{III} can interchange places with a hopping matrix element, t, that describes the electron transfer. The *t-J* model is the simplest model that incorporates these two key processes and can be used to handle concepts as the quantum spin liquid, resonating valence bond state, Zhang-Rice singlet etc [4, 5]. For details of the very interesting and extensively investigated field of electronic and magnetic properties of the doped cuprate superconductors the reader is referred to Refs. [1] to [12].

In this study we will restrict ourselves to magnetic properties of some nominally integer valence cuprates and oxychlorides. Even under this restriction a large variety of phenomena of copper magnetism has been reported and many problems are still unsolved. To start with the consideration of single Cu ions is suggested by the mentioned above fact that, due to strong electron correlation, a description by simple bands of independent electrons will definitely fail. The copper ions experience the influence of their anionic (or more or less

covalent) anisotropic environment in the solid. Hence, even in this most simple approximation the magnetic properties will be anisotropic. In a more careful analysis the interaction between the magnetic ions in the solid have to be considered. Different types of magnetic anisotropy have to be taken into account and to be distinguished from the anisotropy connected with the (quasi) low dimensionality. The next step is to find a relevant spin Hamiltonian in order to describe and to predict the magnetic properties of the considered material. In the approximations needed for this purpose, the (quasi) dimensionality of the system has carefully to be treated because it is known to have crucial influence on the magnetic properties.

2. IONIC COMPOUNDS AS A SIMPLIFIED PICTURE

As already discussed in the previous section, Mott-Hubbard insulators are expected to be well described by electrons being localized on atoms or ions [13]. We will first consider the electronic and magnetic properties of free ions. If a magnetic field H is applied to an ion its quantum mechanical states will be modified resulting in small negative or positive contributions to its magnetic moment, known as diamagnetism or van Vleck paramagnetism, respectively. Additionally, if the atomic shells of the ions are only partially filled by electrons a magnetic moment may occur which does not vanish for $H \rightarrow 0$. This magnetic moment is closely related to the angular momentum of the ion which is a good quantum number because the ion is a rotationally symmetric object. Strictly speaking there are three types of angular momentum quantum numbers: total spin, S, total orbital momentum, L, and total momentum, J, the values of which are well determined by three Hund's rules [13]. As indicated in Table I the first two Hund's rules that determine S and L are a result of the intraatomic electron correlation (due to Coulomb repulsion) whereas the third rule is based on spin-orbit interaction. In the solid cuprate structure the copper ions experience an interaction with their anionic environment characterized by (i) electrostatic interactions (crystal fields) and (ii) overlap of wave functions resulting in (indirect) exchange interaction with neighbor Cu ions and covalence effects based on hybridization of various electronic configurations [14]. Covalency manifests itself by remarkable deviations of the oxidation state (or valence) here represented by a Roman number, for example Cu^{II}, from the real charge represented by arabic superscripts, for example Cu^{2+}, where by definition the oxygen in cuprates has the oxidation state O^{-II} [15]. As a result of the covalence effects the cuprates are charge transfer insulators rather than conventional Mott-Hubbard insulators i.e. the gap separating the Hubbard subbands is of the order of the Cu-to-O hole transfer energy ($\varepsilon_p - \varepsilon_d$) instead of the Coulomb interaction strength at the copper sites, U_d [14]. Due to the interaction effects the second and third Hund's rules will be violated and in particular the orbital angular momentum L is said to be quenched i.e. it disappears because the interaction of the copper ion with the solid strongly violates rotational symmetry. On the other hand, the first Hund's rule still fairly works in certain compounds i.e. the total spin remains a good quantum number (exceptions will be discussed in Section 2.3) and the mentioned above interactions of the Cu ions result in anisotropic properties of the spin based magnetization as will be discussed in Section 2.2. For well understood reasons, Cu^{I} cuprates are usually characterized by a two-fold coordination i.e. they contain CuO_2 dumbbells (see Fig. 3), whereas the typical topological unit of Cu^{II} cuprates is a planar square CuO_4 plaquette forming one or two dimensional networks and, as

Table I. Hunds' rules determining the total spin S, orbital angular momentum L and the total angular momentum J, applied to copper ions: 1. $S \rightarrow$ maximum (Coulomb repulsion); 2. $L \rightarrow$ maximum (Coulomb repulsion); 3. $J = L + S$ (spin-orbit coupling)

Ion	Single electron configurations	S	L	J
Cu^{+}	$3d^{10}$	0	0	0
Cu^{2+}	$3d^{9}$	1/2	2	5/2
Cu^{3+}	$3d^{8}$	1	3	4

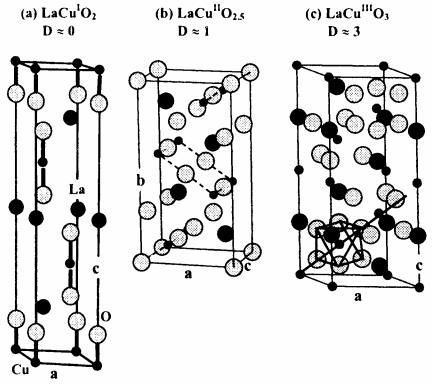

Fig. 3. Change of valence and crystal structure by oxidation. D is the (quasi) dimensionality of the lattice structure. (a) $LaCuO_2$ (SG: $R\bar{3}m$) – isolated O-Cu^{I}-O dumbbells in the delafossite structure. (b) $La_2Cu_2O_5$ (SG: *Pbam*) – two-leg ladder with Cu^{II}. (c) $LaCuO_3$ (SG: $R\bar{3}c$) is a distorted perovskite

shown in Fig. 3, Cu^{III} cuprates can also crystallize in three-dimensional structures [15-17]. The well defined coordination configurations (with low coordination numbers) also indicate the high degree of covalency in the crystal binding of cuprates.

2.1 Cu^{I} COMPOUNDS

The CuO_2 dumbbells of Fig. 3a with a copper site that is linearly coordinated by two oxygen ions is typical for Cu^{I} cuprates. In some cases the dumbbells are found to be isolated as in $LaCuO_2$ with delafossite type structures (see Fig. 3a), but the dumbbells can also be connected forming rings as in KCuO or chains as in CsCuO, or they build two-dimensional networks as for example in $K_3Cu_5O_4$ [17]. These dumbbell structures can neither be described by ionic crystal binding nor by pure sp bonding (assuming a completely filled Cu 3*d* shell). Rather than *s-d* hybridization has to be taken into account [18]. On the other hand, concerning their magnetic and electrical-transport properties the Cu^{I} cuprates behave as expected in the simple ionic picture: they are diamagnetic insulators [17]. Detailed data on the magnetic and electronic properties of the Cu^{I} cuprates are rare in literature because these compounds are considered to be much less interesting than Cu^{II} compounds which may become superconducting if doped.

As can be seen in Fig. 3 the formal oxidation state of $LaCuO_2$ can be increased from I to II or III by increasing the oxygen stoichiometry from 2 to 2.5 or 3.

2.2 Cu^{II} COMPOUNDS

The magnetic properties of cuprates with two-valent copper, Cu^{II}, have been extensively investigated because among them are the undoped parent compounds of high-T_c superconductors containing two-dimensional networks of corner-shared CuO_4 plaquettes as shown in Fig. 1. Most of these compounds are insulators and the ionic picture describing Cu^{II} as a $S = 1/2$ ion (see Table I) works rather well. The contribution of such an ion to the magnetization is

$$\mu = gS\mu_B \approx 1\,\mu_B,$$

where $g \approx 2$ is the g factor or Landé factor of an ion with vanishing (i.e. totally quenched) orbital momentum L. The contribution of the same ion to Curie paramagnetism is

$$\mu_p = g\sqrt{S(S+1)}\,\mu_B \approx 1.73\,\mu_B \tag{2}$$

The difference between μ and μ_p is due to quantum effects and it has its maximally achievable value for $S = 1/2$. In cuprates the Cu^{II} magnetic moments dominantly interact with their next Cu neighbors via indirect exchange interaction through oxygen. Therefore these materials are often considered as ideal model systems for spin 1/2 quantum magnetism that can well be described by Heisenberg type Hamiltonians as

$$H = J\sum_{(i,j)} \boldsymbol{S}_i\boldsymbol{S}_j \tag{3}$$

where (i, j) is over nearest-neighbor bonds and $\boldsymbol{S}_i\boldsymbol{S}_j$ is the scalar product of the quantum operators of spin 1/2 vectors. In the typical Cu-O-Cu straight bonds of corner-shared plaquettes (as in Fig. 1) the coupling is strongly antiferromagnetic ($J/k_B \approx 1500$ K) and results

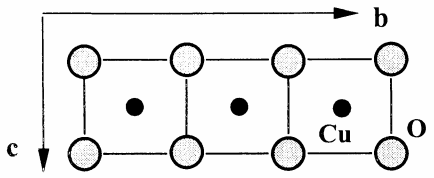

Fig. 4. Edge-sharing CuO_4 plaquettes forming chains in Li_2CuO_2 [19, 20]

from hybridization of the oxygen $2p_\sigma$ orbitals with the neighboring $3d$ Cu orbitals (superexchange). In the large family of Cu^{II} cuprates there are also cases where the indirect exchange through oxygen is not along straight lines [17]. Examples are compounds with edge-sharing CuO_4 plaquettes as in Li_2CuO_2 (Fig. 4) or compounds with more or less isolated plaquettes as in La_2BaCuO_5 (Fig. 5). In these cases the strength of the exchange interaction is reduced and J may even be negative (ferromagnetic coupling) [22-25].

Magnetic order and ground states in quasi low-dimensional Cu^{II} cuprates

All materials including cuprates are three-dimensional magnetic systems. However, as discussed above, the strength of exchange interaction between the magnetic moments in Cu^{II} cuprates strongly depends on the local topology and the angle of Cu-O-Cu bonds. Therefore Cu^{II} cuprates usually consist of relatively weakly exchange-coupled subsystems with a dimen-

sionality D lower than 3 where the exchange coupling within the subsystem is relatively strong. To some approximation such materials can be considered as being of (quasi low) dimensionality D [26]. In this sense the compounds of Figs. 1 are of $D \approx 2$, those of Figs. 4 and 6 of $D \approx 1$ and that of Fig. 5 of $D \approx 0$. Many rigorous theoretical results on magnetic properties of low-dimensional Cu^{II} cuprates have been derived by analysing the spin 1/2 Hamiltonian (3). For $J < 0$ and arbitrary dimensionality $D = 0$, 1, 2 or 3 the ground state can easily be shown to be ferromagnetic with totally aligned individual moments, each with its maximum value of 1 Bohr magneton. The direction of the collective magnetization can be fixed by a very small external field or a weak magnetic anisotropy. With increasing temperature, the magnetization decreases and vanishes at the Curie temperature T_c. However, a finite T_c (in the order of $|J|/k_B$) only exists for $D = 3$, whereas T_c is zero for $D < 3$ i.e. at finite temperatures ferromagnetic order cannot exist in finite clusters, linear chains or square

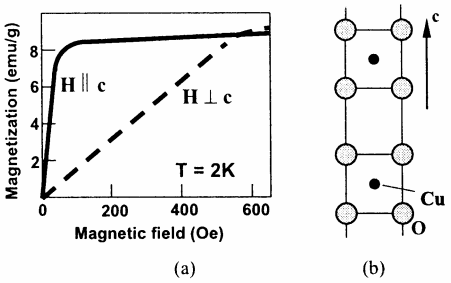

Fig. 5. The ferromagnet La_2BaCuO_5 (space group $P4/mbm$). (a) The demagnetization curves clearly indicate ferromagnetism, where the tetragonal c-axis is the magnetically easy direction. Curie temperature $T_c \approx 6.5$ K [21]. (b) CuO_4 plaquettes (parallel to the tetragonal c-axis) as typical for Cu^{II} cuprates

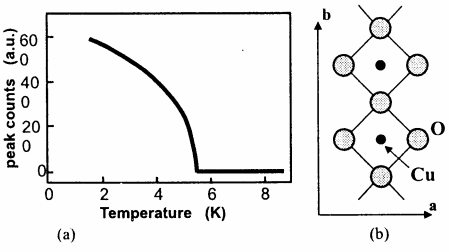

Fig. 6. The $D = 1$ (chain) compound Sr_2CuO_3. (a) Temperature dependence of the intensity of the (0, 1/2, 1/2) neutron diffraction peak, which is proportional to the staggered magnetization [27]. (b) Corner-sharing CuO_4 plaquettes along the b axis (SG: $Immm$)

lattices [28]. In the case of antiferromagnetic coupling ($J > 0$) in Eq. (3) the situation is more complicated. Now, even at $T = 0$ finite clusters as well as linear chains are in a singlet state i.e. the Cu^{II} sites do not exhibit any individual magnetic moments. The difference between the two systems is that in finite clusters ($D = 0$) the magnetic excitations are separated from the singlet ground state by a finite gap [29] called spin gap whereas for $D = 1$ there is no spin gap [30]. On the other hand for $D = 3$ [31] as well as the square lattice ($D = 2$) [32] a Néel type antiferromagnetic order with a staggered magnetization on the individual Cu^{II} sites has been theoretically shown to exist in the quantum mechanical ground state. Due to quantum fluctuations the individual staggered moment per Cu^{II} site in the square lattice ($D = 2$) is about $0.6\,\mu_B$ instead of the full value of Eq. (1) [33]. Because the Néel type order violates the rotational symmetry of the Hamiltonian (3) there must exist zero-energy Goldstone modes (spin waves) and consequently there is no spin gap in that case [34]. For the simplest $D = 0$ cluster, namely a dimer of two interacting spin 1/2 moments, the spin gap and the susceptibility χ can easily be calculated [35]. Upon cooling the antiferromagnetically coupled

dimers from a high temperature, χ will increase similar as in a Curie paramagnet. On the other hand, the spin gap causes $\chi = 0$ at $T = 0$. Consequently, the temperature dependence of χ has a maximum as shown in Fig. 7. The maximum in $\chi(T)$ is a typical feature of low-dimensional Heisenberg antiferromagnets independent of the existence or non-existence of a spin gap (see Figs. 7 and 8). Two-leg spin ladders (as that in Fig. 3b), or more generally even-number leg ladders, show a spin gap and an exponential decay of spin-spin correlations. Their coherent singlet ground state is considered to be a realization of the quantum spin liquid or resonating valence bond state proposed by Anderson [4]. It has been shown that the spin gap opens immediately upon introduction of non-zero interchain coupling J' (see Fig. 7)) within the lad-

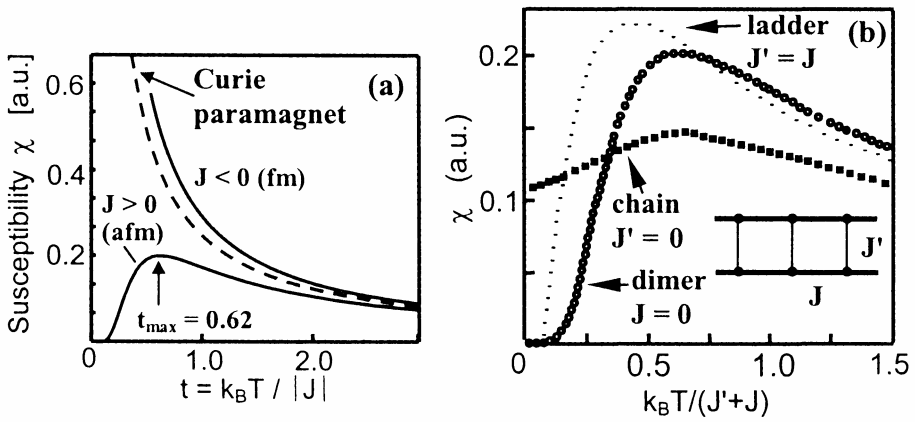

Fig. 7. Temperature dependence of the susceptibility of spin 1/2 Hamiltonians (3) [3]. (a) Dimer ($D = 0$). (b) Dimer ($D = 0$), chain ($D = 1$) and a two-leg spin ladder

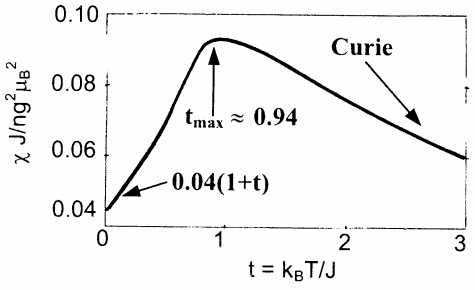

Fig. 8. Susceptibility of the square-lattice spin 1/2 Heisenberg antiferromagnet, where n is the volume density of the spin 1/2 moments [3]

ders [36]. On the other hand, odd-number leg ladders (including uncoupled chains as that of Fig. 6) have a slow decay of spin-spin correlations and no spin gap [37].

Dimensionality crossover and quantum critical points in Cu^{II} cuprates

Contrary to the discussed above theoretical predictions concerning the magnetic properties of low-dimensional magnetic systems, many quasi-low-dimensional Cu^{II} cuprates show long-range magnetic order and magnetic phase transitions at finite temperatures (as e.g. shown in

Figs. 2, 5 and 6). It is generally accepted that the reason for these observations is the (relatively small) exchange interaction between Cu^{II} magnetic moments of the nearly separated low-dimensional subsystems. For quasi $2D$ Cu^{II} cuprates (as the undoped parent compounds of typical high-T_c superconductors (see Figs. 1 and 2)) Soukoulis et al. derived the formula

$$k_B T_N = \frac{4\pi J}{3 \ln (32 J/J_\perp)} \tag{4}$$

using low-temperature spin wave theory [38]. In Eq. (4) T_N is the Néel temperature, J is the main antiferromagnetic exchange interaction (within the plaquettes of Fig. 1) and $J_\perp$ is the interplanar antiferromagnetic exchange interaction. This approximation works rather well for rhombohedral La_2CuO_4 where the typical data are $T_N \approx 300$ K, $k_B J \approx 1500$ K and $J_\perp/J \approx 10^{-5}$ [3]. Thus at high enough temperature the influence of $J_\perp$ is negligible and the quasi-low-dimensional materials behave as really low-dimensional ones. For example, the layered Cu^{II} cuprates will show a temperature dependence of susceptibility χ as shown in Fig. 8 which however is difficult to be observed because the maximum of χ and the Curie-type behavior will occur at temperatures as high as or even higher than 1500 K [3]. At sufficiently low temperatures the influence of $J_\perp$ results in $3D$ magnetic ordering as presented in Fig. 2 and described by Eq. (4). Also a crossover from decreasing χ with decreasing temperature (as expected from Fig. 8 for $t < t_{max}$) to a special behavior of $\chi(T)$ connected with $3D$ ordering has been observed for La_2CuO_4 [39]. Such a dimensionality crossover upon cooling from lower to higher dimensionality has often been observed in quasi-low-dimensional materials [26].

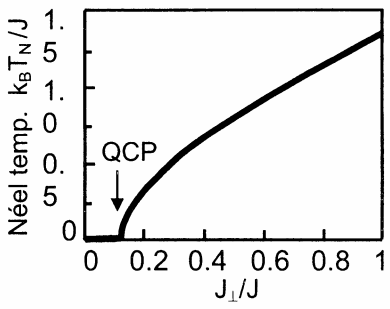

Fig. 9. Néel temperature T_N of interacting two-leg ladders. $J_\perp$ is the strength of the coupling between the ladders, J the coupling strength along the legs and along the rungs of the ladders. QCP marks the quantum critical point at $J_\perp \approx 0.12\,J$ [42]

A variation of the exchange coupling $J_\perp$ between low-dimensional subsystems can result in further phenomena that have to be distinguished from the dimensionality crossover discussed above. In the following this will be discussed for the two-leg ladder material $La_2Cu_2O_5$ (see Fig. 3b) [40]. As a good approximation, in that case, the coupling along the rungs of the ladder (J' in Fig. 7b) can be considered to be equal to the coupling J along the legs [41]. Although the single ladder clearly has dimensionality $D = 1$ its behavior remarkably deviates from that of a single chain i.e. it is a spin liquid with a spin gap resulting in zero susceptibility at zero temperature (see Fig. 7b). If now an interaction $J_\perp$ (of the same strength as J) is switched on the system will be a $3D$ antiferromagnet with staggered magnetic

moments at the Cu^{II} sites and a gapless spin-wave spectrum. Thus an interesting question is how the system transforms between the magnetically ordered state and the spin-liquid state if $J_\perp$ is varied between 0 and J. It was shown by quantum Monte Carlo simulations that the spin gap opens below a critical interladder coupling $J_\perp \approx 0.11J$ [41]. This value can be considered as a quantum critical point [32] characterizing the quantum phase transition between the ordered state and the spin liquid. Using and generalizing the bond-operator mean-field theory the Néel temperature of the system could be calculated for the whole range $0 \leq J_\perp \leq J$ (see Fig. 9) and a critical value $J_\perp/J \approx 0.12$ was found [42]. At intermediate temperatures the system crosses over to the $1D$ decoupled-ladders regime. However, for interladder coupling $J_\perp$ below its critical value, $0.12J$ no crossover to $3D$-type ordering does occur at low temperatures.

Magnetic anisotropy in Cu^{II} cuprates

In condensed matter a Cu^{II} site has always a discrete environment of neighbors, i.e. anions or cations etc., which represent a local anisotropy. In crystalline solids the local anisotropy adds up to the macroscopic crystalline anisotropy which is manifested by anisotropic physical properties of the considered material. In the previous subsection we discussed the directional dependence of the strength of exchange interactions, resulting in quasi-low dimensionality which is a special type of anisotropy. Note that low dimensionality has to be distinguished from real magnetic anisotropy which is the subject of this subsection. For example, the Heisenberg Hamiltonian (3) is isotropic i.e. rotationally symmetric also for chains ($D = 1$) or square lattices ($D = 2$). Magnetic anisotropy is the dependence of magnetic properties on the direction (with respect to the crystal axes). A typical example is the directional dependence of demagnetization curves shown in Fig. 5.

As discussed above the magnetic moment on a Cu^{II} site is based on the copper spin and therefore the anisotropy of the solid can be transmitted to the magnetization only by spin-orbit (LS) interaction or by magnetic dipolar interaction which however can be neglected in most cases. Thus in any approach to magnetic anisotropy in Cu^{II} cuprates LS coupling has to be explicitly taken into account. Lets first consider the magnetic anisotropy on a single Cu^{II} site. Usually crystalline-electric-field (CEF) splitting in cuprates is large compared to both k_BT (temperature) and LS coupling. Therefore the orbitally non-degenerated CEF ground state with quenched orbital angular momentum and two-fold spin degeneracy is a good zero order approximation. The LS coupling (of strength λ) and the Zeman energy can be considered as a perturbation

$$H_1 = \lambda \boldsymbol{L}\boldsymbol{S} + \mu_B \boldsymbol{H}(2\boldsymbol{S} + \boldsymbol{L}) \tag{5}$$

Collecting the terms proportional to the field $\boldsymbol{H}$ from the result of first and second order perturbation theory results in an effective Zeman energy

$$H_{\text{eff}} = \sum_{\mu\nu} 2\mu_B H_\mu (\delta_{\mu\nu} - \lambda\Lambda_{\mu\nu}) S_\nu \tag{6}$$

with

$$\Lambda_{\mu\nu} = \sum_n \frac{\langle 0|L_\mu|n\rangle\langle n|L_\nu|0\rangle}{E_n - E_0}, \tag{7}$$

where E_n and $|n\rangle$ are the CEF energy levels and eigenfunctions, respectively, and L_μ are the components of the orbital angular momentum operator. Taking into account Eq. (6) the g factor (1) has to be replaced by the g tensor

$$g_{\mu\nu} = 2(\delta_{\mu\nu} - \lambda\Lambda_{\mu\nu}). \tag{8}$$

For Cu^{II} in elongated tetragonal surroundings with C_{4v} symmetry the second term in Eq. (8) is positive and typical values of $g_{\mu\nu}$ are $g_{zz} = 2.20$ and $g_{xx} = g_{yy} = 2.08$ [35]. The increase of g (> 2) is due to an induced orbital momentum which arises from mixing with higher-energy orbital states due to the *LS* coupling. The g tensor (8) represents the magnetic anisotropy of a single Cu^{II} magnetic moment. The perturbation term proportional to λ^2 contributes to magnetic anisotropy only for $S > 1/2$. Therefore it is not effective for Cu^{II} moments.

A further type of magnetic anisotropy in Cu^{II} cuprates is superexchange modified by *LS* coupling, which is usually much more efficient than the anisotropy of g. In Hamiltonians as that in Eq. (3) the spin is present only in order to fulfill the Pauli principle. Therefore Hamiltonians describing pure exchange interactions are invariant under rotations in spin space [29]. Taking the *LS* coupling on two neighboring Cu^{II} sites, together with the isotropic superexchange between them, as a perturbation to the same non-perturbed states as considered above for the calculation of the g tensor, perturbation theory results in the following spin Hamiltonian that has to be added to the isotropic Hamiltonian (3)

$$H_a = \alpha_{DM} J \sum_{(i,j)} \mathbf{d}_{ij}(\boldsymbol{S}_i \times \boldsymbol{S}_j) + \alpha_{xy} J \sum_{(i,j)} \mathbf{S}_i^z \mathbf{S}_j^z \tag{9}$$

where $\alpha_{DM} \sim\lambda$ and $\alpha_{xy} \sim\lambda^2$ and $\boldsymbol{d}_{ij}$ are vectors depending on the bond (i, j) and the symmetry of its environment [12, 13, 43]. The first term in Eq. (9), the Dzyaloshinsky-Moriya type anti-symmetric exchange interaction, was introduced by Dzyaloshinsky [44]. The second term in Eq. (9) may result in a Kosterlitz-Thouless phase transition even if the (i, j) in Eqs. (3) and (9) run over a $2D$ square lattice [45]. The $2D$ low-temperature Kosterlitz-Thouless phase does not carry a staggered magnetization. However it is generally accepted that the xy term in Eq. (9) together with the interlayer coupling $\alpha_\perp = J_\perp/J$ (see previous subsection) results in a $3D$ xy transition which is assumed to assist the development of Néel type magnetic order in tetragonal layered Cu^{II} cuprates as $Sr_2CuO_2Cl_2$ where $\alpha_\perp << \alpha_{xy}$ [46, 47]. This approach results in the following expression for the Néel temperature of layered cuprates

$$T_N = \frac{0.3\,\pi k_B J}{\ln(4\,\alpha_{eff}/[0.3\,\pi^2 \ln(4\,\alpha_{eff}/\pi)])} \tag{10}$$

with $\alpha_{eff} = 4\alpha_{xy} + 2\alpha_\perp$ [47, 12].

Weak ferromagnetism in $Ba_2Cu_3O_4Cl_2$

The lattice structure $Ba_2Cu_3O_4Cl_2$ contains two Cu sites, Cu_A and Cu_B (see Fig. 10a). The Cu_A ions form the typical, for Cu^{II} compounds, planar Cu_AO_4 plaquettes which build

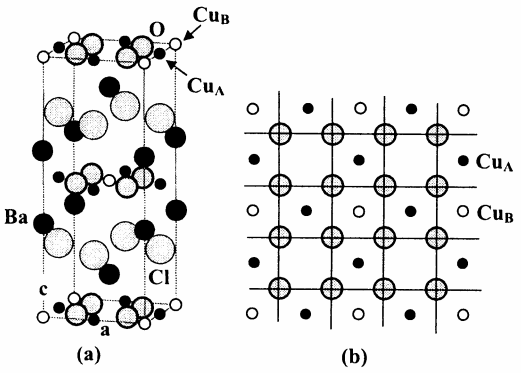

Fig. 10. Crystal structure of the Cu^{II} compound $Ba_2Cu_3O_4Cl_2$ [48]. (a) unit cell (space group: *I4/mmm*). (b) planar network of corner-sharing Cu_AO_4 plaquettes and isolated Cu_BO_4 plaquettes. The Cu_BO_4 plaquettes share their edges with those of the Cu_AO_4 plaquettes

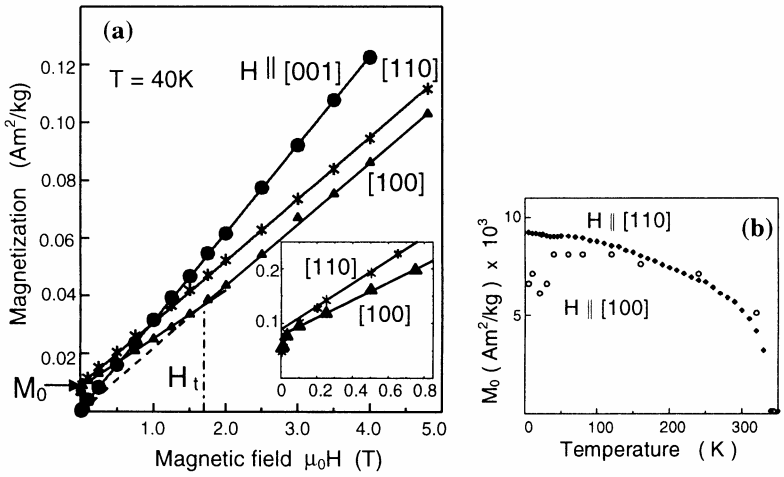

Fig. 11. (a) Magnetization *vs.* field curves for $Ba_2Cu_3O_4Cl_2$. For applied fields H parallel to [110] or [100] a small residual magnetization M_0 is observed. For H parallel to [100] a kink is found at a threshold field H_t. Above H_t the magnetization curves for [110] and [100] are parallel to each other. (b) Temperature dependence of M_0 [51]

a planar corner-sharing network (Fig. 10b). The Cu_B ions fill half of the remaining empty oxygen squares. Therefore, the magnetic behavior of this compound is expected to be that of a 2*D* quantum Heisenberg antiferromagnet. For all Cu_A sites the bond angle Cu_A-O-Cu_A is 180°, whereas the angle for the Cu_A-O-Cu_B bonds is 90° and the Cu_B-Cu_B interaction is expected to be very small. Two antiferromagnetic ordering temperatures are observed: At $T_{NA} \approx 337$ K the Cu_A ions order antiferromagentically, whereas the Cu_B ions order at a quite lower temperature $T_{NB} \approx 33$ K [49-51]. As the magnetization *versus* field curves for applied fields parallel to the [001] direction pass the origin (see Fig. 11a), the easy direction of the staggered magnetization is in the (*a, b*) plane. The finite magnetization, M_0, measured for

$H \to 0$ in both directions in the basal plane, [100] and [110], indicates the presence of a small spontaneous magnetization [50-52]. Furthermore, some metamagnetic behavior i.e. a small kink of the $M(H)$ curve at a threshold field H_t is found for $H\|$ [100]. At higher fields the demagnetization curve measured for $H\|$ [100] (cf. Fig. 11a) approaches a straight line passing through the origin. The temperature dependence of the residual magnetization M_0, measured for $H \|$ [100] and $H \|$ [110], is given in Fig. 11b. Typical hysteresis loops measured for $H \|$ [100] are presented in Fig. 12. Above the lower Néel temperature T_{NB} the coercive field H_c is more than one order of magnitude smaller than below. Between T_{NB} and T_{NA} $\mu_0 H_c$ is only about 0.5 mT, for both directions [110] and [100], and does not much depend on temperature [51].

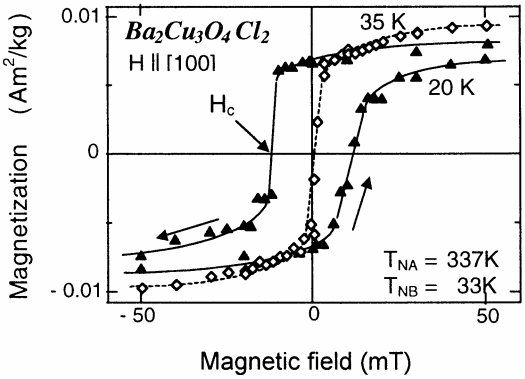

Fig. 12. Above T_{NB} a residual net magnetization but (nearly) no hysteresis is observed. Below T_{NB} where the Cu_B moments are also antiferromagnetically ordered, a hysteresis is found as typical for ferromagnets [51]

An anisotropic pseudodipolar interaction between the antiferromagnetically ordered Cu_A and the paramagnetic Cu_B moments has been successfully proposed [52, 53] to explain the presence of a spontaneous magnetization and the metamagnetic behavior of $Sr_2Cu_3O_4Cl_2$ which is very similar to that of $Ba_2Cu_3O_4Cl_2$. A quasi-dipolar field caused by the ordered Cu_A moments is assumed to induce a net moment in the Cu_B subsystem.

Spin flop transition in $Ba_3Cu_2O_4Cl_2$

The structure of $Ba_3Cu_2O_4Cl_2$ is orthorhombic (space group *Pmma*; see Fig. 13). The two Cu sites, Cu_A and Cu_B, within the unit cell and the surrounding oxygen ions form nearly regular squares. However, these plaquettes are edge-sharing and build folded chains. The axes of the chains are parallel to the orthorhombic *a*-axis. The field dependence of the magnetization, M, measured along the *a*-axis is shown in Fig. 14a. Below $T_N \approx 20$ K these $M(H)$ curves show a metamagnetic transition i.e. a strong upward curvature in a limited range of the magnetic field H. At a threshold field, H_t of about 2.6 T the M *vs.* H curves measured at low temperatures jump between two straight lines. Above the jump, the slope is considerable larger than below. Whereas M, and thereby the susceptibility χ, increases nearly linearly with increasing temperature at fields below H_t and below T_N, above H_t only a weak dependence on temperature is observed. No such jump of the magnetization has been found for $\vec{H} \| b$ or c (cf. Fig. 14b). These observations indicate a spin-flop transition [56] in the case $\vec{H} \| a$ i.e. a transition from a collinear antiferromagnetic structure with localized moments aligned along the easy *a*-axis to a configuration perpendicular to the field. From $K_1 = H_t^2(\chi_\perp - \chi_\|)/2$ [13]

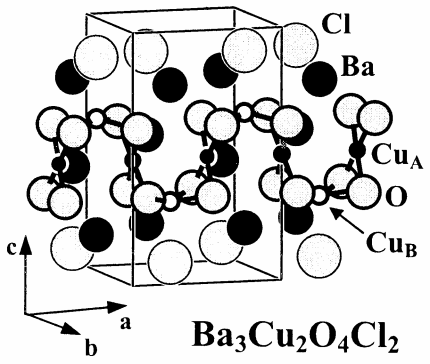

Fig. 13. Crystal structure of the folded-chain compound $Ba_3Cu_2O_4Cl_2$ (*SG Pmma*) with two types of Cu^{II}-sites, Cu_A and Cu_B [54]

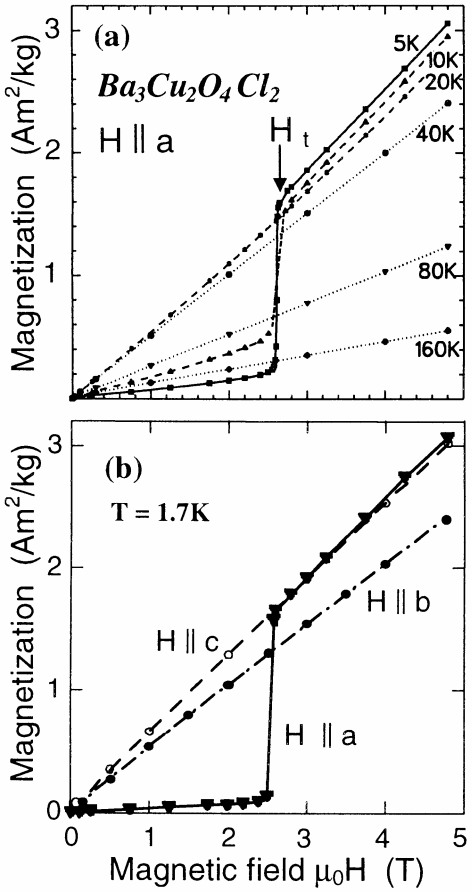

Fig. 14. (a) For fields H applied parallel to the a-axis, below the Néel temperature $T_N \approx 20$ K: spin flop transition characterized by a threshold field H_t. Above T_N: paramagnetic behavior. (b) For H parallel to the b – or c-axis: no spin-flop [51, 55]

with the susceptibilities measured in fields parallel ($\chi_\parallel$) and perpendicular ($\chi_\perp$) to the easy a-axis the corresponding anisotropy constant is estimated to be $K_1 \approx 1.1 \cdot 10^4$ VAs/m^3 ($T = 1.7$ K). Above the spin-flop transition the moments progressively rotate towards the field

direction. In that field range the increase of M is mainly determined by exchange interaction and therefore only weakly depends on temperature. The spin structure of $Ba_3Cu_2O_4Cl_2$ has not yet been determined experimentally. From symmetry arguments it follows that (i) the moments of crystallographically equivalent Cu moments are parallel and (ii) the moments of the non-equivalent sites are antiparallel. Thus, despite the presence of well separated one-dimensional CuO_2 chains in this compound it behaves as a classical $3D$ antiferromagnet. This can be explained by its electronic structure and its influence on the magnetic properties [57, 58].

2.3 Cu^{III} compounds

As shown in Fig. 15 the ionic compound Cs_3CuF_6 contains isolated $Cu^{III}F_6$ octahedra and it is an ideal Curie paramagnet with a paramagnetic moment of 3 Bohr magnetons per copper site [59]. This is in good agreement with the ionic approximation which predicts $S = 1$ (see Table I) and $\mu_p = 2.8\ \mu_B$ (see Eq. (2)) for Cu^{III} ionic compounds.

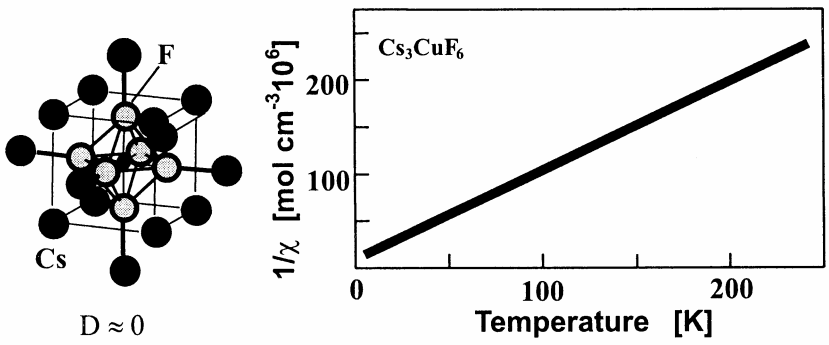

Fig. 15. (a) Local environment of Cu^{III} in Cs_3CuF_6: The Cu^{3+} ion is surrounded by an ideal octahedron of 6 F^- ions. These octahedrons are isolated in the crystal structure, i.e. Cs_3CuF_6 can be considered as quasi zero dimensional. (b) The inverse-susceptibility *vs.* temperature curve shows that Cs_3CuF_6 is an ideal *Curie* paramagnet [59]

A net oxidation state Cu^{III} can also be realized in cuprates. But, so far, these compounds are not intensely investigated because in the high-T_c superconductor scene they are considered as overdoped Cu^{II} cuprates which do not show superconductivity. A common feature of the Cu^{III} cuprates is that they do not have a magnetic moment corresponding to $S = 1$. Various mechanisms, in principle, could be responsible for the Cu^{III} magnetic moment to disappear. The first mechanism is zero-field splitting resulting in the $S_z = 0$ ground state which can occur e.g. in tetragonal crystalline electric fields. For temperatures small compared to the energy difference of the $S_z = 0$ and the $S_z = \pm 1$ level, an $S = 1$ system will behave like an $S = 0$ (singlet) system [35]. On the other hand, low-spin states occur if the crystal-field splitting of the single-electron levels is strong compared to the intraatomic interaction normally ensuring

the 1st Hund's rule. A subset of lower crystal-field levels will be filled violating 1st Hund' rule and, consequently, the total spin vanishes [60]. In recent years a further concept has been generally accepted for doped cuprates which explicitly takes into account the observed presence of a hole near the oxygen sites and the high degree of covalency in these compounds. According to this model a hole on the copper site forms a singlet, called Zhang-Rice singlet [61], with a second hole being located on (and shared by) the surrounding oxygen ions. Among the Cu^{III} cuprates diamagnetic insulators, as e.g. $LiCuO_2$ [62], as well as metals with Pauli paramagnetism as e.g. $LaCuO_3$ [63] have been found. The crystal structure of $LaCuO_3$ is shown in Fig. 3c.

3. SUMMARY AND CONCLUSIONS

This study was restricted to copper magnetism in integer-valence cuprates (and copper oxyhalogenides). A natural and important extension would be to consider also rare-earth containing cuprates (where La is substituted by 4*f* elements) and mixed-valence compounds containing strongly correlated itinerant *d* electrons. Even under the mentioned above limitation the cuprates show a large variety of magnetic phenomena originating from the *d*-electrons of copper in the oxidation states Cu^{I}, Cu^{II} or Cu^{III}. The ionic approximation for the Cu species, describing oxidation states by charge states works fairly well. According to this approximation the ground state of Cu^{+} compounds has no magnetic moment and they exhibit diamagnetism or van Vleck paramagnetism. The orbital angular momentum of Cu^{II} and Cu^{III} is quenched due to crystalline-electric-field effects and covalency. Cu^{2+} has an odd number of *d*-electrons i.e. it is a so called Kramers ion with a doubly degenerated ground state. Its paramagnetic moment is well approximated by the spin-only value of 1.73 Bohr magnetons. The magnetic moment of Cu^{3+} in cuprates is usually zero (low spin) due to a higher degree of covalency. The Cu^{III} cuprates, in particular their magnetic properties, are not much investigated so far. Concerning the linkage of the copper sites by overlapping wave-functions (in the localized-electron picture) or by dispersion of energy bands (in the description by itinerant electrons) most of the cuprates can be considered as quasi-two or one or zero dimensional systems. The majority of published experimental and theoretical results on copper magnetism concern the quasi-two dimensional Cu^{II} cuprates because they contain most of the undoped parent compounds for high-T_c superconductors. In the ionic approximation the overlap of wave functions results in exchange interactions of the magnetic moments which may lead to antiferromagnetic or ferromagnetic long-range order. As an alternative the low-temperature behaviour can be governed by spin-singlet ground states which can be separated from excited (magnetic) states by non-zero or zero gaps. In the case of cuprates the dominating type of interaction is antiferromagnetic superexchange via oxygen anions. Therefore the mentioned parent compounds of high-T_c superconductors can be considered, in a good approximation, as 2*D* square lattice Heisenberg antiferromagnets. However, for understanding the Néel type magnetic ordering of these materials at finite temperatures the crossover to dimensionality three, mediated by interlayer exchange coupling of strength $\alpha_{\perp}$, and to Kosterlitz-Thouless type ordering due to symmetric anisotropic exchange (strength α_{xy}), have to be taken into account. These crossover phenomena are not yet well understood. Progress in this field will depend on whether a successful combination of analytical approaches with

computational modeling can be developed. One of the main aims of this research will be to establish complete T-$\alpha_{\perp}$-α_{xy}-phase diagrams. A further problem is how Dzyaloshinsky-Moriya type interaction modifies these phase diagrams or causes spin canting that may result in weak ferromagnetism or weak antiferromagnetism. A promising modification of the layered cuprates is to break-up the CuO_2 planes into weakly coupled ladders. Such spin ladders can be used to study quantum phase transitions and crossover phenomena between dimensionality 0, 1, 2 and 3.

References

[1] J. G. Bednorz, K. A. Müller, Z. Phys. **B64**, 189 (1986).
[2] P. Fulde, Electron *Correlations in Molecules and Solids*, Springer, Berlin (1995).
[3] D.C. Johnston, *Normal-State Magnetic Properties of Single-Layer Cuprate High-Temperature Superconductors and Related Materials*, in: K. H. J. Buschow (ed.), *Handbook of Magnetic Materials*, Elsevier, Amsterdam, vol. 10, p. 1 (1997).
[4] P. W. Anderson, Science **235**, 1196 (1987).
[5] T. M. Rice, Physica C **282-287**, xix-xxiii (1997).
[6] R. P. Norman, and C. Pépin, cond-mat/032347 (17 February 2003).
[7] J. M. Tranquada, B. J. Sternlieb, J. D. Axe, Y. Nakamura, S. Uchida, Nature **375**, 561 (1995).
[8] N. Nücker, J. Fink, B. Renker, D. Ewert, C. Politis, P. J. W. Weijs, J. C. Fuggle, Z. Phys. **B67**, 9 (1987).
[9] E. Dagotto, Rev. Mod. Phys. **66**, 763 (1994).
[10] J. González, M. A. Martín-Delgado, G. Sierra, A. H. Vozmediano, *Quantum Electron Liquids and High-T_c Superconductivity*, Springer, Berlin (1995).
[11] P. W. Anderson, *The Theory of Superconductivity in the High-T_c Cuprates*, Princeton University Press, Princeton NJ (1997).
[12] M. A. Kastner, R. J. Birgeneau, G. Shirane, Y. Endoh, Rev. Mod. Phys. **70**, 897 (1998).
[13] K. Yosida, *Theory of Magnetism*, Springer Series in Solid State Sciences 122, Springer, Berlin (1996).
[14] J. Zaanen, and G. A. Sawatzky, J. Sol. State Chem. **88**, 8 (1990).
[15] A. W. Sleight, Science **242**, 1519 (1988).
[16] Hk. Müller-Buschbaum, Angew. Chemie **101**, 1503 (1989).
[17] Hk. Müller-Buschbaum, Angew. Chemie **103**, 741 (1991).
[18] A.W. Sleight, Physica C **162-164**, 3 (1989).
[19] W. Losert, R. Hoppe, Z. anorg. allg. Chem. **515**, 95 (1984).
[20] Y. Mizuno, T. Tohyama, S. Maekawa, T. Osafune, N. Motoyama, H. Eisaki, S. Uchida, Phys. Rev. B **57**, 5326 (1998).
[21] F. Mizuno, H. Masuda, I. Hirabayashi, S. Tanaka, M. Hasegawa, U. Mizutani, Nature **345**, 788 (1990).
[22] S. Tornow, O. Entin-Wohlman, Aharony, Amnon, Phys. Rev. **B60**, 10206-10215 (1999).
[23] P. W. Anderson, Phys. Rev. **79**, 350 (1950).
[24] J. B. Goodenough, Phys. Rev. **100**, 564 (1955).
[25] J. Kanamori, J. Phys. Chem. Sol. **10**, 87 (1959).
[26] L. J. de Jongh, *Magnetic Properties of Layered Transition Metal Compounds*, Kluwer Academic Publishers, Dordrecht (1990).
[27] K. M. Kojima, Y. Fudamoto, M. Larkin, G. M. Luke, J. Merrin, B. Nachumi, Y. J. Uemura, N. Motoyama, H. Eisaki, S. Uchida, K. Yamada, Y. Endoh, S. Hosoya, B. J. Sternlieb, G. Shirane, Phys. Rev. Lett. **78**, 1787 (1997).
[28] N. D. Mermin, and H. Wagner, Phys. Rev. Lett. **17**, 1133 (1966).
[29] D. C. Mattis, *The Theory of Magnetism*, Harper & Row, New York (1965).
[30] H. Bethe, Z. Physik **71**, 205 (1931).
[31] T. Kennedy, E. H. Lieb, B.S. Shastry, J. Stat. Phys. **53**, 1019 (1988).

[32] S. Chakravarty, B. I. Halperin, D. R. Nelson, Phys. Rev. B **39**, 2344 (1989).
[33] E. Manousakis, Rev. Mod. Phys. **63**, 1 (1991).
[34] H. Wagner, Z. Physik **195**, 273 (1966).
[35] O. Kahn, *Molecular Magnetism*, VCH Publishers, New York (1993).
[36] T. Barnes, E. Dagotto, J. Riera, E. S. Swanson, Phys. Rev. **B47**, 3196 (1993).
[37] E. Dagotto and T. M. Rice, Science **271**, 618 (1996).
[38] C. M. Soukoulis, S. Datta, Y. H. Lee, Phys. Rev. **B44**, 446 (1991).
[39] D. C. Johnston, T. Matsumoto, Y. Yamaguchi, Y. Hidaka, and T. Murakami, Magnetic Susceptibility Anisotropy in High T_c Cuprates, in: T. Oguchi, K. Kadowaki, and T. Sasaki (eds.), *Electronic Properties and Mechanisms of High T_c Superconductors*, Elsevier, Amsterdam, pp. 301-306 (1992).
[40] Z. Hiroi, and M. Takano, Nature **377**, 41 (1995).
[41] M. Troyer, M. E. Zhitomirsky, K. Ueda, Phys. Rev. **B55**, R6117 (1997).
[42] B. Normand, and T. M. Rice, Phys. Rev. **B56**, 8760 (1997).
[43] T. Moriya, Phys. Rev **120**, 91 (1960).
[44] I. J. Dzyaloshinsky, J. Phys. Chem. Sol. **4**, 241 (1958).
[45] J. M. Kosterlitz, and D. J. Thouless, J. Phys. C: Sol. State Phys. **6**, 1181 (1973).
[46] M. Matsuda, K. Yamada, K. Kakurai, H. Kadowaki, T. R. Thurston, Y. Endoh, Y. Hidaka, R. J. Birgeneau, M. A. Kastner, P. M. Gehring, A. H. Moudden, G. Shirane, Phys. Rev. **B42**, 10098 (1990).
[47] B. Keimer, A. Aharony, A. Auerbach, R. J. Birgeneau, A. Cassanho, Y. Endoh, R. W. Erwin, M. A. Kastner, G. Shirane, Phys. Rev. **B45**, 7430 (1992).
[48] R. Kipka, and Hk. Müller-Buschbaum, Z. anorg. allg. Chem. **419**, 58 (1976).
[49] K. Yamada, N. Suzuki, Y. Akimitsu, Physica B **213&214**, 191 (1995).
[50] T. Ito, H. Yamaguchi, K. Oka, Phys. Rev. **B55**, R684 (1997).
[51] D. Eckert, K. Ruck, M. Wolf, G. Krabbes, K.-H. Müller, J. Appl. Phys. **83**, 7240 (1999).
[52] F. C. Chou, Aharony, Amnon, R. J. Birgeneau, O. Entin-Wohlman, M. Greven, A. B. Harris, M. A. Kastner, Y. J. Kim, D. S. Kleinberg, Y. S. Lee, Q. Zhu, Phys. Rev. Lett. **78**, 535 (1997).
[53] B. Parks, M. A. Kastner, Y. J. Kim, A. B. Harris, F. C. Chou, O. Entin-Wohlman, Aharony, Amnon, Phys. Rev. **B63**, 134433 (2001).
[54] R. Kipka, and Hk. Müller-Buschbaum, Z. anorg. allg. Chem. **422**, 231 (1976).
[55] M. Wolf, K. Ruck, D. Eckert, G. Krabbes, K.-H. Müller, J. Magn. Magn. Mater. **196-197**, 569 (1999).
[56] L. Néel, Ann. Phys. (Paris) **5**, 232 (1936).
[57] K.-H. Müller, and M. Wolf, J. Appl. Phys. **87**, 6022 (2000).
[58] V. Yushankai, M. Wolf, K.-H. Müller, R. Hayn, H. Rosner, Phys. Rev. **B62**, 14229 (2000).
[59] R. Hoppe, and G. Wingefeld, Z. anorg. allg. Chem. **519**, 195 (1984).
[60] S. G. Vulfson, *Molecular Magnetochemistry*, Gordon and Breach Science Publishers, Australia (1998).
[61] F. C. Zhang, and T. M. Rice, Phys. Rev. **B37**, 3759 (1988).
[62] T. Mizokawa, A. Fujimori, H. Namatame, K. Akeyama, N. Kosugi, Phys. Rev. **B49**, 7193 (1994).
[63] J.-S. Zhou, W. Archibald, J. B. Goodenough, Phys. Rev **B57**, 2017 (1998).